Structure, magnetic properties and Mossbauer spectra of $RTiFe_{11}C_x$ (R=Y and Gd)

1993 J. Phys.: Condens. Matter 5 3027

(http://iopscience.iop.org/0953-8984/5/18/025)

J. Phys.: Condens. Matter 5 (1993) 3027–3038. Printed in the UK

Structure, magnetic properties and Mössbauer spectra of $RTiFe_{11}C_x$ (R = Y and Gd)

Z W Li, X Z Zhou and A H Morrish
Department of Physics, University of Manitoba, Winnipeg, Canada R3T 2N2

Received 4 January 1993

Abstract. The carbides $RTiFe_{11}C_x$ (R=Y and Gd) have been prepared by heating powders of $RTiFe_{11}$ in CH_4 at 500 °C. For both the C concentration is about $x = 0.7$–0.8 on the basis of the weighing method and Mössbauer spectra. X-ray diffraction indicates that these carbides retain the crystal structure of their parents, but the cell volume expands by about 3%. The Curie temperatures increase by 175 and 100 °C, respectively, as compared to those of their parents. The ratio of the relative change of the Curie temperature to the relative change of the cell volume, $\rho = (\Delta T_c/T_c)/(\Delta V/V) = 12.4$, is a constant for $YTiFe_{11}C_x$ annealed at various temperatures. This result indicates that the increase of the Curie temperature is a volume effect. Mössbauer spectra at room temperature are fitted using seven subspectra for $YTiFe_{11}C_{0.7}$ and $GdTiFe_{11}C_{0.7}$, because the C atoms affect the hyperfine parameters. Their average hyperfine fields are 30.2 and 29.1 T, respectively, which is an increase of 30 and 15% as compared to those for the parents.

1. Introduction

Many researchers have found it interesting that some atoms can enter interstitial sites of RFe compounds and modify their magnetic properties. Coey and co-workers [1,2] first prepared a new series of interstitial rare-earth iron nitrides, $R_2Fe_{17}N_x$, by reacting powders of small R_2Fe_{17} particles with NH_3 or N_2 at about 500 °C. Later the method was extended to prepare $RTiFe_{11}N_x$ compounds [3]. Both $R_2Fe_{17}N_x$ and $RTiFe_{11}N_x$ retain their parent's crystal structure, but the cell volumes expand when interstitial N atoms are present. Neutron diffraction showed that the N atoms occupy the 9e site for the Th_2Zn_{17} structure, the 6h site for the Th_2Ni_{17} structure [4,5] and the 2b site for the $ThMn_{12}$ structure [6].

As for N atoms, the C atoms also enter interstitial sites after heating the powders of the rare-earth iron compounds in a hydrocarbon [7,8]. In this paper, the carbides $RTiFe_{11}C_x$ (R = Y and Gd) were prepared by heating powders of $RTiFe_{11}$ at 500 °C in CH_4. Their crystal structure and Curie temperatures were measured. Mössbauer spectra were collected and analysed, with the object of unraveling the magnetic properties of these carbides on an atomic scale.

2. Experiment

$RTiFe_{11}$ (R = Y and Gd) were prepared by arc-melting of better than 99.5% pure primary materials in a purified argon atmosphere followed by annealing at 1100–1200 K for 72 h in an Ar atmosphere and then quenching in air. The $RTiFe_{11}$ compounds were ground into fine-particle powders (the size of the particles was smaller than 20 μm). The powders were

0953-8984/93/183027+12$07.50

heated in CH_4 in a pressure of about two bars at various temperatures for one hour. Then the sample chamber was pumped for a few minutes to eliminate any H_2. Powders heated at 500 °C were annealed in an Ar atmosphere for five hours in addition to the above heating process. By weighing, the C concentration was determined to be $x = 0.8(2)$, $0.5(2)$ and $0.1(1)$ for the sample $YTiFe_{11}$ annealed at 500, 450 and 400 °C, respectively.

X-ray diffraction experiments were performed with a diffractometer using Cu K_α radiation. Curie temperatures were obtained with a vibrating sample magnetometer in an applied field of 0.050 T.

^{57}Fe Mössbauer spectra of the $RTiFe_{11}C_x$ compounds were taken at room temperature using a conventional constant-acceleration spectrometer. The γ-ray source was ^{57}Co in a Rh matrix. Mössbauer absorbers were powdered samples with about 8 mg cm^{-2} of natural iron. Calibration was made by using the spectrum of α-Fe at room temperature. Since the quadrupole splitting was much smaller than the magnetic hyperfine field splitting for all samples, a perturbation Hamiltonian was used to analyse the Mössbauer spectral data. The parameters obtained for each six-line pattern by a least-squares fitting procedure were the magnetic hyperfine field, B_{hf}, the quadrupole splitting, ϵ, the isomer shift, δ, the line widths and intensities. The relative areas for the six lines of a subpattern were constrained to be in the ratio 3 : 2 : 1 : 1 : 2 : 3, respectively.

3. Results

3.1. Crystal structure

X-ray diffraction patterns show that all samples ($RTiFe_{11}$, R = Y and Gd), annealed in CH_4 at 500 °C for one hour, retain the $ThMn_{12}$ structure. The cell volumes increase by about 3% as compared to those for their parents. Since the radius of a C atom is smaller than that of a rare-earth or an Fe atom, an increase of the lattice parameters implies that the C atoms enter the interstitial positions in the lattice rather than substituting for the rare-earth or Fe atoms. In addition, small amounts of α-Fe are found in all carbide samples. The lattice parameters a and c for the carbides $RTiFe_{11}C_x$ (R = Y and Gd) annealed at about 500 °C are listed in table 1.

Table 1. Lattice parameters and Curie temperatures for $RTiFe_{11}$ and $RTiFe_{11}C_x$ (R = Y and Gd) annealed in CH_4 at 500 °C for one hour.

	a (Å)	c (Å)	c/a	V (Å^3)	$\Delta V/V$ (%)	T_c (°C)
$YTiFe_{11}$	8.539(3)	4.806(3)	0.563	350		250(5)
$YTiFe_{11}C_x$	8.572(4)	4.893(4)	0.571	360	2.9	425(5)
$GdTiFe_{11}$	8.547(8)	4.802(6)	0.562	351		335(5)
$GdTiFe_{11}C_x$	8.583(8)	4.908(8)	0.571	361	3.1	435(5)

Some typical x-ray diffraction patterns for $YTiFe_{11}$ powders annealed in CH_4 in various temperatures for one hour are shown in figure 1. The lattice parameters, a and c, are plotted against the annealing temperature, T_a, in figure 2. For a sample annealed at a temperature of 400 °C, these lattice parameters change but little compared to the unheated parent. For samples annealed at 450 °C, the diffraction lines broaden and two sets of diffraction patterns are observed (see in figure 1(b)). One is close to the pattern for untreated $YTiFe_{11}$, the other to the pattern for the sample annealed at 500 °C. For the sample annealed at 500 °C,

the lattice parameters a and c have increased significantly; it is found that the cell volume expands from 350 Å^3 to about 360 Å^3. At the annealing temperature of 550 °C, the lattice parameters a and c are the same as those for the sample annealed at 500 °C, but the amount of α-Fe increases. This shows that C absorption has reached saturation. When the heating temperature is 750 °C, the $RTiFe_{11}C_x$ decomposes completely into α-Fe and a rare-earth carbide.

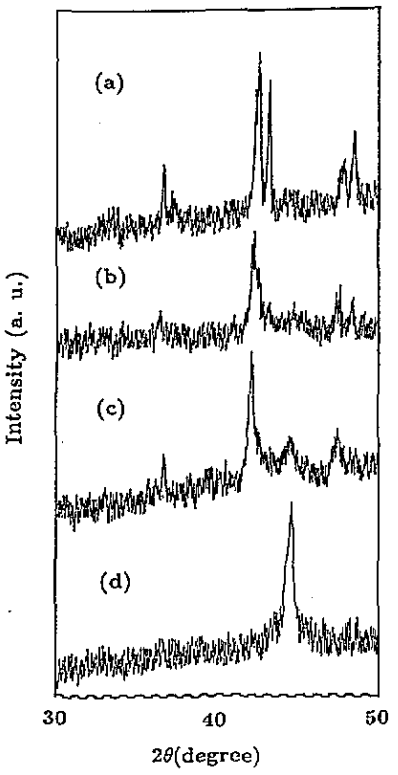

Figure 1. Diagrams of x-ray diffraction patterns of $YTiFe_{11}$ with no heating (*a*) and after heating in CH_4 at two bars for one hour at (*b*) 450 °C (*c*) 500 °C and (*d*) 750 °C.

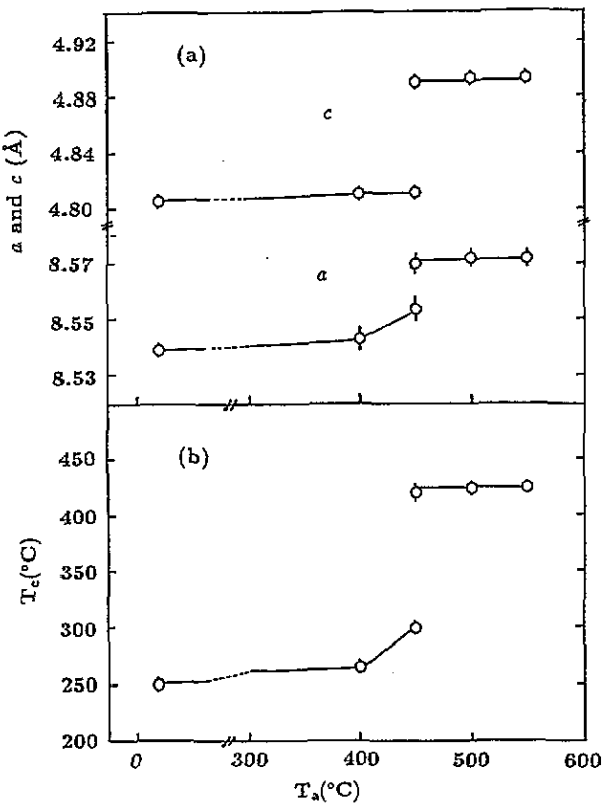

Figure 2. (*a*) Lattice parameters and (*b*) Curie temperatures for $YTiFe_{11}$ after heating at various temperatures, T_a, in CH_4 at two bars for one hour.

3.2. Curie temperature

The Curie temperatures increase with the cell volume expansion in the C absorption process, as shown in table 1. Some typical thermomagnetic scans are shown in figure 3. The dependence of the Curie temperatures on the annealing temperature of the samples is shown in figure 2(*b*) for $YTiFe_{11}$. The Curie temperature, T_c, is 250 °C for virgin $YTiFe_{11}$ and has a rapid increase for the samples annealed above 450 °C. For the sample annealed at 450 °C, there exist two Curie temperatures, one at 300 °C and the other at 420 °C. The origin is an insufficient amount of C absorption. Higher and lower Curie temperatures correspond to two parts of a particle, respectively. One is rich in C absorption, probably near the surface,

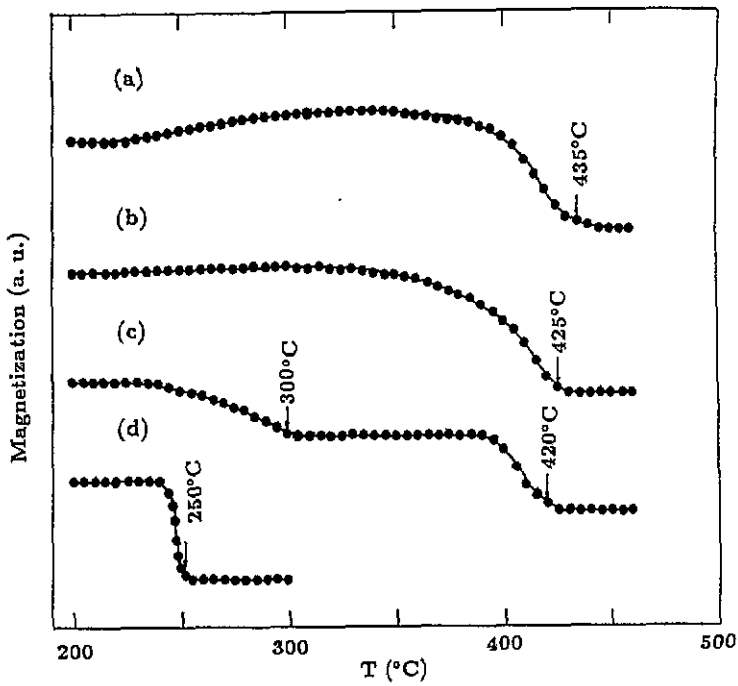

Figure 3. Some typical thermomagnetic scans. (*a*) $GdTiFe_{11}$ after heating at 500 °C in CH_4 at two bars for one hour; (*b*) $YTiFe_{11}$ after the same heat treatment; (*c*) $YTiFe_{11}$ after heating at 450 °C in CH_4 at two bars for one hour; and (*d*) unheated $YTiFe_{11}$.

and the other, probably the core, has a small C content. For samples annealed at 500 and 550 °C, only one Curie temperature of 425 °C is observed. Apparently, these samples have sufficient absorption to have a uniform C concentration.

4. Mössbauer spectra

4.1. Mössbauer spectra at room temperature

The Mössbauer spectra at room temperature for $RTiFe_{11}$ (R = Y and Gd) powders after heating at 500 °C in CH_4 for one hour are shown in figure 4. For $RTiFe_{11}C_x$, a good fit with three subspectra, as used for the parent materials, can no longer be obtained. The source is the influence of the C atoms on the hyperfine parameters. It was found necessary to divide the patterns for each site into two or three components that correspond to the various C neighbour configurations. In addition, an α-Fe and a doublet spectrum were introduced. For $GdTiFe_{11}C_x$, a weak six-line spectrum with an isomer shift of $-0.2\,mm\,s^{-1}$ and a hyperfine field of 22.9 T is also included. The amount is about 5%, based on the spectral area.

The assignments of the subspectra for $RTiFe_{11}C_x$ are determined by the following considerations. (i) The relative areas of each subspectrum should roughly be equal to the probability of the binomial distribution of C atoms. (ii) Based on the sequence of the hyperfine fields for $RTiFe_{11}$ and $RTiFe_{11}N_x$, the hyperfine fields for $RTiFe_{11}C_x$ are also considered to be in the order $B_{hf}(8i) > B_{hf}(8j) > B_{hf}(8f)$. On the basis of those two

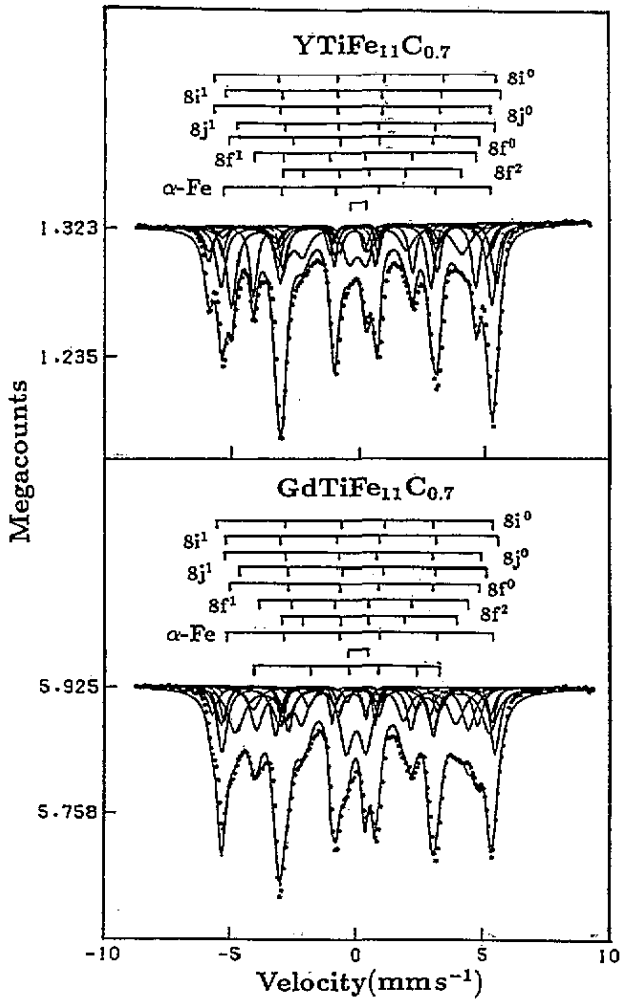

Figure 4. Mössbauer spectra at room temperature and the computer fitted curves for (*a*) $YTiFe_{11}C_{0.7}$ and (*b*) $GdTiFe_{11}C_{0.7}$.

principles, the most suitable assignments of the subspectra for the carbides R = Y and Gd are shown in table 2, where the 8z in $8z^k$ represents an 8i, 8j or 8f site and the superscript k represents the number of nearest-neighbour C atoms surrounding a particular z site.

It is assumed that the C atoms occupy a 2b site in the $ThMn_{12}$ structure, which is the same as for N atoms. The 8i and 8j sites have one 2b site as their nearest neighbour and the 8f site has two 2b sites. According to the binomial distribution model, the probability of finding m C atoms in n nearest-neighbour 2b sites for a particular Fe site, $P(m, n; x)$, is given by

$$P(m, n; x) = \frac{n!}{m!(n-m)!} x^m (1-x)^{n-m} \tag{1}$$

where x is the C concentration. The relative areas of the Mössbauer subspectra are close to the probabilities $P(m, n; x)$ with $x = 0.7$. Hence, the C concentration is estimated to

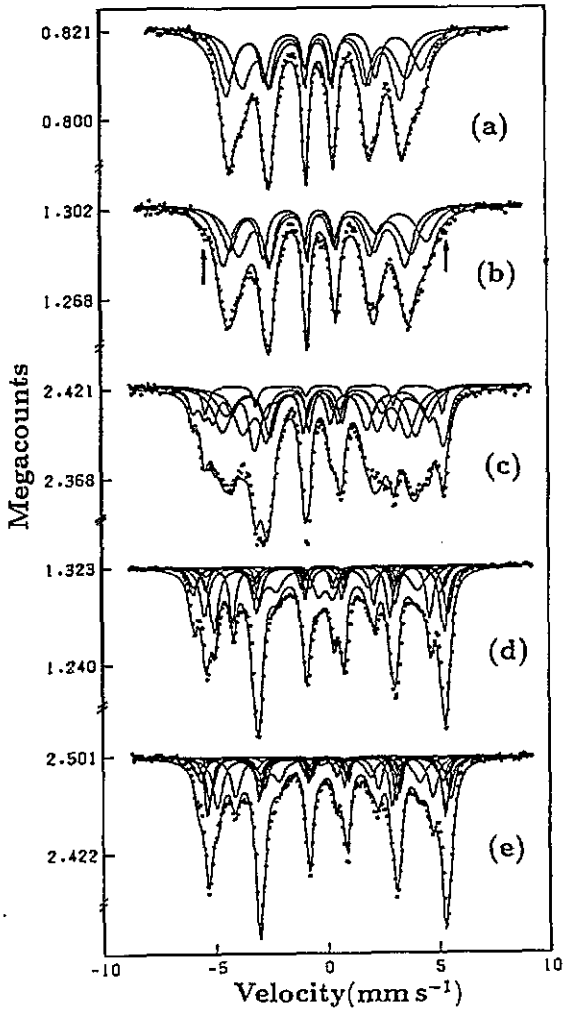

Figure 5. Mössbauer spectra at room temperature and computer fitted curves for $YTiFe_{11}$ before (*a*) and after heating at various temperatures in CH_4 at two bars for one hour, (*b*) 400 °C, (*c*) 450 °C, (*d*) 500 °C and (*e*) 550 °C.

be 0.7 and the chemical formula is written as $RTiFe_{11}C_{0.7}$. The value is consistent with $x = 0.8(2)$ obtained from weighing.

The adjacent C atoms have a large influence on the hyperfine parameters of an Fe nucleus. The hyperfine fields decrease with an increase in the adjacent C atoms. These properties are similar to those observed for the compounds Fe_xC_y and Fe_xN_y. For example, the average hyperfine fields are 20.8 and 18.0 T for the isostructural Fe_3C and Fe_5C_2, respectively [9]. Further, Mössbauer spectral analysis for Fe_4N indicates that the hyperfine fields are 34.1 and 21.7 T for zero and two adjacent N atoms, respectively [10]. In addition, the effect of the adjacent C atom on the hyperfine field is much larger for the 8f site than for the 8i and 8j sites. The hyperfine field for the 8f site decreases by about 5 T per one adjacent C atom, whereas it only decreases by about 0.3–2 T for the other two sites. The increase of the isomer shift with adjacent C atoms can be attributed to the transfer of electrons. Since the electronegativity is much larger for C than for Fe, the C atoms have a tendency to attract

Table 2. Hyperfine parameters of $RTiFe_{11}C_x$ (R = Y and Gd) at room temperature. Here B_{hf} is the hyperfine field, ϵ the quadrupole splitting and δ the isomer shift (relative to α-Fe at room temperature). A is the relative area of a Mössbauer subspectrum (the total area of all subspectra is taken as 1) and $P(m, n; x)$ is the probability calculated from equation (1) with $x = 0.7$.

	Site	B_{hf} (T)	ϵ (mm s^{-1})	δ (mm s^{-1})	A	$P(m, n; x)$
$YTiFe_{11}C_x$	$8i^0$	34.9(3)	−0.26(2)	−0.17(2)	0.08(1)	0.08
	$8i^1$	34.0	0.09	−0.03	0.19(2)	0.19
	$8j^0$	34.3	−0.32	−0.25	0.11(2)	0.11
	$8j^1$	32.1	0.27	0.02	0.25(4)	0.26
	$8f^0$	31.2	−0.29	−0.19	0.03(2)	0.03
	$8f^1$	27.5	0.65	−0.07	0.16(3)	0.15
	$8f^2$	22.2	0.68	0.20	0.18(3)	0.18
$GdTiFe_{11}C_x$	$8i^0$	34.2(3)	−0.32(2)	−0.14(2)	0.09(1)	0.08
	$8i^1$	33.6	0.19	−0.09	0.20(2)	0.19
	$8j^0$	31.6	−0.24	−0.24	0.11(1)	0.11
	$8j^1$	31.3	0.14	0.08	0.23(3)	0.26
	$8f^0$	31.2	−0.30	−0.19	0.02(1)	0.03
	$8f^1$	26.2	0.50	−0.12	0.17(3)	0.15
	$8f^2$	21.7	0.60	0.05	0.18(3)	0.18

the conduction electrons of Fe. A decrease in the Fe conduction electrons when the number of adjacent C atoms increases will produce an increase in the isomer shift. In addition, it is also noted that the quadrupole splitting is negative for those subspectra that correspond to no adjacent C atoms and is positive for those subspectra that correspond to one or two adjacent C atoms.

As compared to 23.1 T for $YTiFe_{11}$, the average hyperfine field for $YTiFe_{11}C_x$ is 30.2 T, an increase of about 30%. However, this value is slightly smaller than the hyperfine field of 32.0 T observed for $YTiFe_{11}N_x$. Similarly, the hyperfine field for $GdTiFe_{11}C_x$ is 29.1 T, which is slightly smaller than that for $GdTiFe_{11}N_x$ but still is a 15% increase over that for $GdTiFe_{11}$.

4.2. Mössbauer spectra for $YTiFe_{11}$ annealed in CH_4 at various temperatures

Mössbauer spectra at room temperature for $YTiFe_{11}$ powders after annealing at various temperatures in CH_4, as well as for the original sample, are shown in figure 6.

For the original sample and the sample after annealing at a temperature of 400°C, a good fit is obtained by using three subspectra, which corresponds to the three Fe sites in the $ThMn_{12}$ structure. The hyperfine field is slightly larger for the sample annealed at 400°C than for the original sample. For the samples heated at 500 and 550 °C, the hyperfine parameters are almost same within the experimental errors. The difference is only the amount of α-Fe, 6% and 18% for the samples annealed at 500 and 550 °C, respectively.

For the sample annealed at 450 °C, the Mössbauer spectrum has the characteristics both of the original (at −4 mm s^{-1} and +3.5 mm s^{-1}) and the sample annealed at 500 °C (at −6 to −5 mm s^{-1} and +5.5 mm s^{-1}). It can be considered to be a summation of two spectra. The fitting method used is the following. A standard pattern, $\{y_i\}(i = 1, 256)$, is set by using the hyperfine parameters of the sample annealed at 500 °C. The other pattern is given by three sets of sextets with Lorentzian line shapes

$$\sum_{j=1} L_{i,j}\left(A_j, \Gamma_j, (H_{hf})_j, \epsilon_j, \delta_j; x_i\right) \tag{2}$$

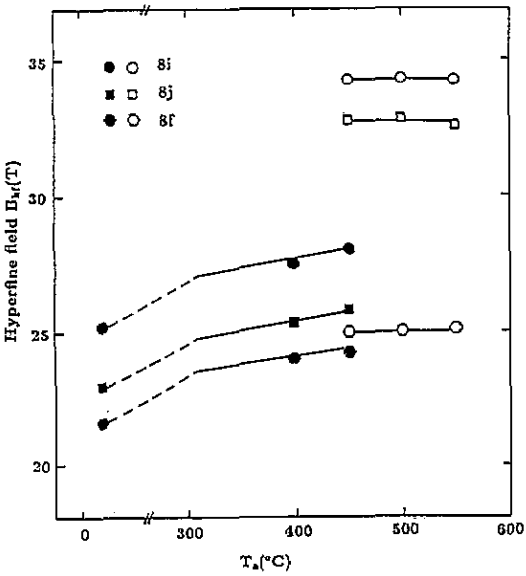

Figure 6. Hyperfine fields at each site for $YTiFe_{11}$ after heating at various temperatures, T_a, in CH_4 at two bars for one hour.

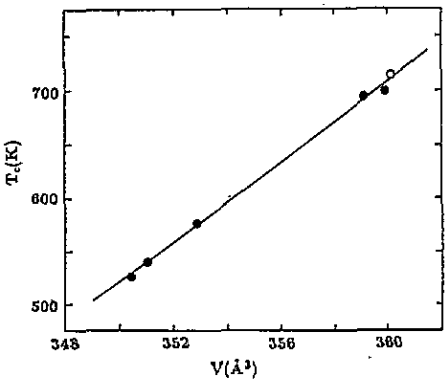

Figure 7. The dependence of the Curie temperature on the cell volume for $YTiFe_{11}C_x$ (the open circle is for $YTiFe_{11}N_x$).

where $L_{i,j}$ is a Lorentz function with the following fitting parameters: intensity A_j, linewidth Γ_j, hyperfine field H_{hf}, quadrupole splitting ϵ_j and isomer shift δ_j; x_i is the channel number. Each sextet corresponds to one Fe site. Thus, the experimental spectrum, $\{Y_i\}(i = 1, 256)$ of the sample heated at 450 °C can be written as

$$Y_i = E - \left(\alpha\{y_i\} - \sum_{j=1} L_{i,j}\left(A_j, \Gamma_j, (H_{hf})_j, \epsilon_j, \delta_j, x_i\right)\right) \tag{3}$$

where E is the average background count and α is a proportionality coefficient for the area ratio of spectrum $y\{i\}$ compared to the total spectrum. A least-squares method was used to fit equation (3). From the fitted results, the areas of the two spectra are 30 and 65%, respectively, and the area of the α-Fe spectrum is 5%.

The hyperfine fields for the samples annealed at various temperatures are plotted in figure 6. The open symbols represent the hyperfine fields of $YTiFe_{11}C_x$ with significant C absorption. The hyperfine fields on a certain site are the same within the experimental errors for the samples annealed between 450–550 °C. The full symbols represent the hyperfine field of $YTiFe_{11}$ with a small C absorptions. The hyperfine field increases for those samples with higher annealing temperature. For the sample annealed at 450 °C, there exist two sets of hyperfine fields.

5. Discussion

5.1. Volume changes and Curie temperatures

The $YTiFe_{11}$ powders annealed in CH_4 at various temperatures have different cell volumes and Curie temperatures. The Curie temperature, T_c, is plotted against the corresponding

cell volume, V, in figure 7. They are almost linear with a slope equal to $18.5\,K\,Å^{-3}$, as obtained from a least-squares fit. A linear dependence of the Curie temperature on the cell volume was also observed for $Y_2Fe_{17}C_x$ and $Gd_2Fe_{17}C_x$ [11].

Let ρ be defined as the ratio of the relative change of the Curie temperature to the relative change of cell volume, i.e.

$$\rho = \frac{\Delta T_c/T_c}{\Delta V/V} = \frac{V}{T_c}\left(\frac{\Delta T_c}{\Delta V}\right). \tag{4}$$

When a slope of $18.5\,K\,Å^{-3}$, a Curie temperature of 523 K and a cell volume of $350\,Å^3$ are substituted into (4) ρ is found to be 12.4 for $YTiFe_{11}$ and its carbides and its nitride.

Experiments have indicated that the pressure dependence of the Curie temperature is linear for a series of RCo and RFe compounds [12]; thus its slope, $\Delta T_c/\Delta P$, is a constant. Now ρ can also be given by the following formulae:

$$\rho = \frac{\Delta T_c/T_c}{\Delta V/V} \tag{5}$$

$$\rho = -\frac{1}{T_c}(\Delta T_c/\Delta P)_V(-V\Delta P/\Delta V)_T \tag{6}$$

$$\rho = -\frac{1}{T_c}\frac{1}{\kappa}(\Delta T_c/\Delta P)_V \tag{7}$$

where $\kappa = -[V(\Delta P/\Delta V)_T)]^{-1}$ is the compressibility of $YTiFe_{11}$. Hence, ρ is expected to be a constant for $YTiFe_{11}C_x$.

For a series of $RTiFe_{11}N_x$ and $RTiFe_{11}C_x$ compounds, the relative change of the Curie temperature, $\Delta T_c/T_c$, is plotted against the corresponding relative change of the volume, $\Delta V/V$, in figure 8. Most of the values are in the range between $\rho = 10$–16. If $(\Delta T_c/\Delta P)_V$ and κ are assumed to be roughly constant for $RTiFe_{11}$ isostructural compounds, this result can reasonably be expected on the basis of (7). In fact, experiments have shown that ρ is roughly constant for other isostructural compounds; for example, $\rho = 0$ for RFe_2, $\rho = 6$–7 for R_6Fe_{23} and $\rho = 11$–13 for R_2Fe_{17} [12]. Figures 7 and 8 suggest that the enhancement of the Curie temperature is a volume effect in $RTiFe_{11}C_x$ and in $RTiFe_{11}N_x$.

5.2. Model of C absorption

The dependences of the lattice parameters, Curie temperatures and hyperfine fields on the annealing temperatures are shown in figure 2(*a*) and (*b*) and figure 5, respectively. There are two characteristics that are common to all three plots. First, for the samples annealed below 450 °C, the lattice parameters, Curie temperatures and hyperfine fields increase only a little as compared to these values for the untreated sample, $YTiFe_{11}$. For the samples annealed at or above 500 °C, these quantities undergo a large increase. Second, for the sample annealed at 450 °C, there exist two sets of hyperfine fields and x-ray patterns and two Curie temperatures. To account for the Mössbauer spectra, and in order to calculate the C distribution in a spherical particle at equilibrium, a C absorption model will now be proposed.

The samples annealed in 500 and 550 °C have sufficient C absorption to become homogeneous $YTiFe_{11}C_{0.7}$, because seven subspectra rather than three spectra are required for a good fit. The increases in the hyperfine field and Curie temperature have their origin in the occupation of C atoms at the interstitial sites. The sample annealed at 400 °C has a

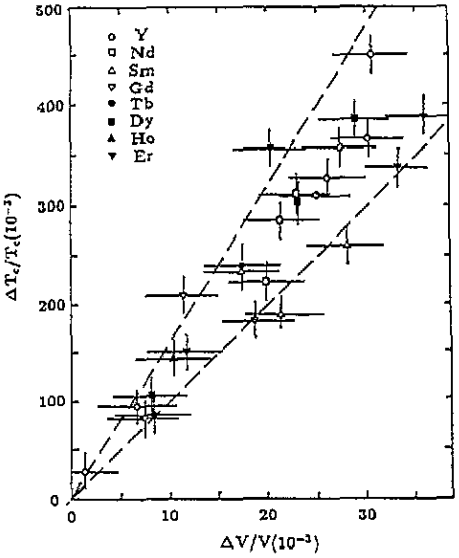

Figure 8. The dependence of the relative change of the Curie temperature on the relative change of the cell volume for $RTiFe_{11}C_x$ and $RTiFe_{11}N_x$ (the data for the Curie temperatures and cell volumes are taken from [3, 13–15]).

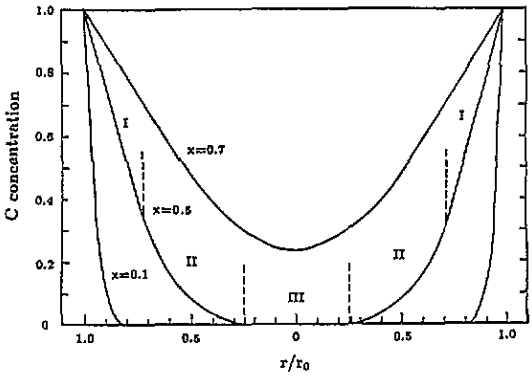

Figure 9. Distribution of C concentration in a spherical particle with $x = 0.7$, 0.5 and 0.1 based on (8).

small C concentration. The chemical formula can be written as $YTiFe_{11}C_{0.1}$, as determined by weighing. For this sample, the particle may have C absorbed only at its surface, because the Mössbauer spectrum can be fitted very well using three subspectra, the same as the untreated sample $YTiFe_{11}$. For the sample annealed at 450 °C, the Mössbauer spectrum has to be fitted using two sets of patterns (see equation (3)). One set is similar to the spectra of the $YTiFe_{11}C_{0.7}$, the other is similar to the spectrum of the $YTiFe_{11}$. From the areas of two sets of patterns, the average C concentration is estimated to be about 0.5, which is consistent with the result obtained from weighing. Thus, the average chemical formula is $YTiFe_{11}C_{0.5}$. Apparently, the particle is not homogeneous on a microscopic scale and can be divided into two parts, one a shell with a rich C absorption and the other a core with a small C absorption. The volume of the two parts are 68 and 32%, respectively, based on the relative areas of the Mössbauer subspectra.

For a spherical particle, a solution of the diffusion equation for a constant concentration on the surface of the particle is given by

$$u(r,t) = u_0 + \frac{2u_0}{\pi(r/r_0)} \sum_{n=1}^{\infty} \frac{(-1)^n}{n} \exp[-(n\pi\ell/r_0)^2] \sin(n\pi r/r_0) \tag{8}$$

where $u(r,t)$ is the equilibrium concentration at a distance r and at a time t, u_0 is the constant concentration at the surface of the spherical particle with a radius of r_0 at the

initial time, and ℓ is the diffusion length. Based on the above equation, three representative distribution curves of C atoms are plotted in figure 9. In the calculation, r_0 and u_0 are taken as 10 μm and 1, respectively; the diffusion length $\ell = (Dt)^{1/2}$, where D is a diffusion coefficient, is taken to be 3.0, 1.7 and 0.4 μm for the three distribution curves, respectively. These values correspond to average C concentrations of $x = 0.70$, 0.50 and 0.10.

A particle may be divided into three regions, based on the slope, dc/dr, of the C concentration against the distance. In region I, the slope is constant, to a good approximation. In region III, the slope is equal to zero. In region II, the slope changes from a constant to zero. For the $x = 0.5$ distribution curve, the three regions have been marked in the figure. The volume and C concentration for each of the three regions have been estimated and the results are listed in table 3.

Table 3. The relative volume, V (in %), and the C concentration (per formula unit) for the three regions of a spherical particle as based on the slope of the C concentration against the particle radius.

	$YTiFe_{11}C_{0.1}$		$YTiFe_{11}C_{0.5}$		$YTiFe_{11}C_{0.7}$	
	V (%)	C	V (%)	C	V (%)	C
Region I	9	0.70	63	0.70	91	0.74
Region II	38	0.12	35	0.18	9	0.32
Region III	53	0	2	0	0	0

For $YTiFe_{11}C_{0.7}$, region I is above 90% of the total volume of the particle. Since the sample is annealed in an Ar atmosphere for five hours after heating in CH_4 at 500 °C for one hour, it seems that almost the whole particle belongs to this region. This region has sufficient C absorbed to produce a large increase in the lattice parameters, Curie temperature and hyperfine field. For $YTiFe_{11}C_{0.5}$, region III can be neglected because its volume is only 2% of the total volume. The C concentration is 0.70 and 0.18 for regions I and II, respectively. Hence, there exist two sets of Mössbauer patterns and x-ray diffraction patterns and two Curie temperatures, one set for the high C concentration region and the other for the low C concentration region. The volume of these two regions is 63 and 35%, respectively, which is consistent with the 68 and 32% obtained from Mössbauer spectra. For $YTiFe_{11}C_{0.1}$, the regions II and III are 38 and 53% of the total volume, respectively. Since region II has a low C concentration (0.12), the difference of the lattice parameters, Curie temperatures and hyperfine fields between the regions II and III is small. Hence, only a slight increase in these parameters are observed. Region I is less than 10% of the total volume, too small to be observed by x-ray diffraction. However, a minor Mössbauer pattern for $YTiFe_{11}C_{0.7}$ might be detectable. Indeed, there may be another subspectrum visible at the wings of the spectrum for $YTiFe_{11}C_{0.1}$, as shown by arrows in figure 5(*b*). These positions are just those for the first and sixth peaks for $YTiFe_{11}C_{0.7}$. The corresponding area is estimated to be about 5%.

6. Conclusions

First, the carbides $RTiFe_{11}C_x$ (R = Y and Gd) have been prepared by annealing powders of $RTiFe_{11}$ in CH_4 at 500 °C. Their C concentration is about $x = 0.7$–0.8 on the basis of both weighing and Mössbauer spectroscopy. These carbides retain the crystal structure of their parents, but the cell volume expands by about 3%.

Second, the Curie temperatures increase by 175 and 100 °C for $YTiFe_{11}C_{0.7}$ and $GdTiFe_{11}C_{0.7}$, respectively, as compared to those for their parents. The ratio of the relative change of the Curie temperature to the relative change of the cell volume, $\rho = (\Delta T_c/T_c)/(\Delta V/V)$, is a constant ($\rho = 12.4$) for $YTiFe_{11}C_x$ with various C concentrations and is in the range of 10–16 for $RTiFe_{11}C_x$ and $RTiFe_{11}N_x$ (R = Y, Nd–Er). These results suggest that the increase in the Curie temperature is a volume effect.

Third, $YTiFe_{11}$ heated at 500 °C in CH_4 for one hour and followed by annealing in an Ar atmosphere has a homogeneous C concentration. For the sample annealed at 450 °C, the particle consists of two parts, one with a rich C concentration and the other with a small C content. This leads to two sets of Mössbauer and x-ray diffraction patterns and two Curie temperatures.

Fourth, Mössbauer spectra at room temperature for $YTiFe_{11}C_{0.7}$ and $GdTiFe_{11}C_{0.7}$ show that the average hyperfine fields are 30.2 and 29.1 T, respectively, which is about a 30 and 15% increase, respectively, as compared to their parents.

Acknowledgments

This work was financed by a grant from the Natural Science and Engineering Research Council of Canada.

References

[1] Coey J M D and Sun Hong 1990 *J. Magn. Magn. Mater.* **87** L251
[2] Sun Hong, Otani Y, Hurley D P F and Coey J M D 1990 *J. Phys.: Condens. Matter* **2** 6465
[3] Yang Y C, Zhang X D, Ge S L, Kong L S, Pan Q, Yang J L, Zhang B S, Ding Y F and Ye C T 1991 *J. Appl. Phys.* **70** 6001
[4] Ibberson R M, Moze O, Jacobs T H and Buschow K H J 1991 *J. Phys.: Condens. Matter* **3** 1219
[5] Yang Y C, Zhang X D, Kong L S, Pan Q, Yang J L, Ding Y F, Zhang B S, Ye C T and Jin L 1991 *J. Appl. Phys.* **70** 6019
[6] Yang Y C, Zhang X D, Kong L S, Pan Q, Ge S L, Yang J L, Ding Y F, Zhang B S, Ye C T and Jin L 1991 *Solid State Commun.* **78** 313
[7] Coey J M D, Sun Hong, Otani Y and Hurley D P F 1991 *J. Magn. Magn. Mater.* **98** 76
[8] Hurley D P F and Coey J M D 1992 *J. Phys.: Condens. Matter* **4** 5573
[9] Bernas H, Campbell I A and Fruchart F 1967 *J. Phys. Chem. Sol.* **28** 17
[10] Nozik A J, Wood J W and Haacke G 1969 *Solid State Commun.* **7** 1677
[11] Liu J P, Bakker K, de Bore F R, Jabcobs T H, de Mooij D B and Buschow K H J 1991 *J. Less-common Met.* **170** 109
[12] Brouha M, Buschow K H J and Miedema A R 1974 *IEEE Trans. Magn.* **MAG-10** 182
[13] Li Z W, Zhou X Z and Morrish A H 1992 *J. Phys.: Condens. Matter* **4** 10409
[14] Liao L X, Altounian and Ryan D H 1991 *J. Appl. Phys.* **70** 6006
[15] Wang Y Z and Hadjipanayis G C 1991 *J. Appl. Phys.* **70** 6009
[16] Williamson D L, Bukshpan S and Ingalls R 1972 *Phys. Rev.* B **6** 4194